

Thermoelectric Generator Performance Enhancement by the Application of Pulsed Heat Power

Samson Shittu, Guiqiang Li, Xudong Zhao, Xiaoli Ma

University of Hull

Cottingham Road, Hull, United Kingdom

S.Shittu@2016.hull.ac.uk; Guiqiang.Li@hull.ac.uk; Xudong.Zhao@hull.ac.uk; X.Ma@hull.ac.uk

Abstract - Thermoelectric generator (TEG) is usually studied under steady state heating conditions however, the use of pulsed heat power could significantly enhance its performance. Therefore, this paper presents a numerical investigation of the thermal and electrical performance of a typical thermoelectric generator (TEG) under both steady state and transient pulsed heating conditions. A three-dimensional finite element model is used to study the temperature, voltage, current distribution and power output of the TEG. A comparison is made between the performance of the TEG under steady state and transient pulsed heating conditions. Furthermore, a parametric study is performed to investigate the influence of thermoelectric leg length and cross-sectional area on the performance of the TEG under both heating conditions. Rectangular and triangular pulsed heat functions are used for the transient study. Results show that rectangular pulsed heating provides the best performance compared to the triangular pulsed heating and steady state heating. In addition, the power output of the TEG decreased as the leg height increased however, it increased as the leg area increased. Therefore, shorter thermoelectric legs with wider cross-sectional area are suggested to enhance the performance of the TEG. This study will provide a valuable reference for future design of thermoelectric generators to obtain optimum performance.

Keywords: Thermoelectric generator, Pulsed heat power, Finite element method, Performance enhancement.

1. Introduction

The world is in urgent need of alternative energy sources contrary to the rapidly depleting widely used fossil fuels which cause several environmental issues like global warming and pollution [1], [2]. Therefore, renewable energy sources are being paid more attention recently due to the unique advantages they offer such as inexhaustibility and low pollution. In automobiles, about 40% of fuel energy is wasted as exhaust gas in the internal combustion engine [3]. Therefore, there is need for a technology that can utilize this waste heat for beneficial use. A thermoelectric generator is solid state device that can generate electricity directly from waste heat via the Seebeck effect as long as there is a temperature difference across its semiconductor materials [4]. Furthermore, thermoelectric generators are small, lightweight and reliable energy converts that operate with no noise or vibration due to the absence of any moving mechanical part [5]. However, even though TEGs are clean energy converters with the aforementioned advantages, their low conversion efficiency and high cost has limited their application widely [6]. Therefore, the research on TEG in recent years has concentrated on optimizing its performance and reducing its costs. The two most widely research methods used to optimize the performance of the TEG are: Geometry optimization and Material optimization [7]. There are several research [8], [9] on optimizing the geometry of thermoelectric generators and results obtained have proven this method to be effective. Furthermore, the optimization of the thermoelectric material is another very significant method to enhance the TEG performance. Generally, a dimensionless parameter known as Figure of merit is used to evaluate the efficiency of the thermoelectric material. The figure of merit, z is defined as by $z = \frac{\alpha^2}{\kappa\rho}$ where, α is the Seebeck coefficient, κ is the thermal conductivity and ρ is the electrical resistivity which all vary with temperature [10]. The best thermoelectric materials are the ones with a high electrical conductivity, low thermal conductivity and high Seebeck coefficient [11].

In terms of geometry optimization, Omer et al. [12] presented a theoretical investigation of a thermoelectric generator with emphasis on optimizing the thermoelectric leg length. The authors stated that the power output of the TEG can be enhanced by optimizing its geometry. Hadjstassou et al. [13] performed an analytical study on the performance of a segmented thermoelectric generator and found that the device achieved a high efficiency of 5.29% at 324.6K temperature difference. Furthermore, Zhang et al. [14] studied the effect of thermoelectric leg geometry configuration on the performance

of an annular thermoelectric generator. Results showed that the maximum power output per nit mass was attained when the leg geometry parameter $m=-1$. In addition, Kossyvakis et al. [15] studied the influence of thermoelectric geometry on the performance of hybrid photovoltaic-thermoelectric system and found that shorter thermoelectric leg lengths enhanced the system performance. Besides the two aforementioned methods, another way to optimize the performance of a thermoelectric generator is by increasing the temperature difference across the TEG. This can be achieved by the use of pulsed heat power instead of the widely used steady state heating.

Therefore, this paper presents the optimization of thermoelectric generator by the use of pulsed heating. This research investigates the influence of transient and steady state heating on the thermal and electrical performance of a thermoelectric generator. Geometry optimization is also performed to determine the optimum thermoelectric leg length and area. A three-dimensional numerical model is developed in COMSOL 5.4 Multiphysics software and finite element method is used to perform the analysis. To the best of our knowledge, this study is the first of its kind and would provide valuable information on the optimization of thermoelectric generators using pulsed heat power. The only pervious similar study was performed by [16] however, temperature dependent thermoelectric material properties were not used and geometry optimization was not performed. In addition, only rectangular pulsed heating was considered in that study. Considering the temperature dependence of thermoelectric materials ensures the accuracy of the results obtained and more realistic simulation. In fact, the power output and efficiency of a thermoelectric generator is affected by the temperature dependency of the thermoelectric material properties [17]. Furthermore, this study is carried out at matched load condition and the heat transfer equations are solved using finite element method (FEM). The advantages of using FEM are: it provides a user-friendly interface for modelling and result analysis while also increasing the simulation result accuracy. More importantly, the use of FEM software like COMSOL allows the coupling of different physical models and performance of a detailed investigation.

2. Geometry Description

The geometry of the studied thermoelectric generator is shown in Fig. 1. It consists of an alumina ceramic for enhancing thermal conductivity, copper conductors used for enhancing electrical conductivity, solder material for reducing thermal stress and a pair of n-type and p-type semiconductors legs. An external load resistor (R_L) is connected to close the circuit and measure power output. In this study, the n-type and p-type thermoelectric legs are of the same dimensions and are made of Bismuth telluride. Bismuth telluride is the best material for low temperature range because of its high figure of merit. Transient and steady state heating conditions are applied to the hot side of the TEG while the cold side is maintained at a constant temperature of 298K. The lower left copper electrode is grounded while the lower right copper electrode is connected to the external resistor to close the circuit. Electrical and thermal contact resistance are ignored, and adiabatic condition is assumed. The geometric dimensions of the thermoelectric generator are shown in Table 1.

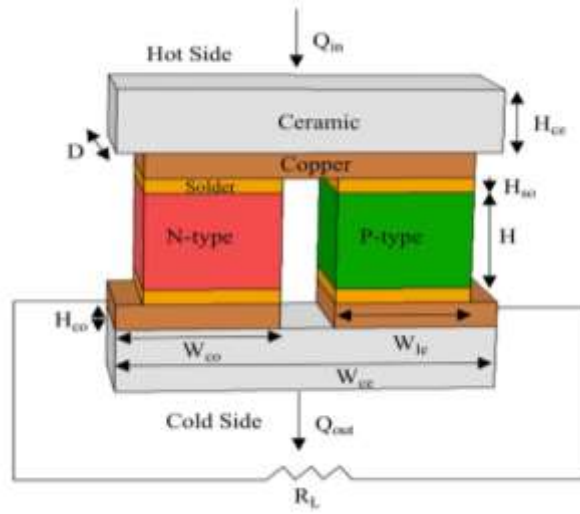


Fig. 1: Schematic diagram of a thermoelectric generator.

Table 1: TEG geometric dimensions.

Parameter	Symbol	Value
Ceramic height	H_{ce}	0.75mm
Solder height	H_{so}	0.175mm
Copper height	H_{co}	0.3mm
Leg height	H	1mm
Ceramic depth	D	1.4mm
Ceramic width	W_{ce}	3.92mm
Leg width	W_{le}	1.4mm
Leg area	A_{le}	1.96mm
Copper width	W_{co}	1.68mm

3. Numerical Model

In this study, the thermoelectric analysis includes the Peltier effect, Fourier effect, Joule effect and Thomson effect. Finite element method is utilized to solve the thermoelectric governing equations using COMSOL 5.4 Multiphysics software. The coupled equation of heat transfer and current density continuity are given as [16]:

$$\rho_d C_p \frac{\partial T}{\partial t} + \nabla \cdot q'' = Q' \quad (1)$$

$$\nabla \cdot J = \frac{\partial \rho_c}{\partial t} \quad (2)$$

where C_p is specific heat capacity, ρ_d is density, t is time, T is temperature, ρ_c is charge density, Q' is Joule heating energy and q'' is the input heat flux.

$$Q' = J \cdot E \quad (3)$$

$$q'' = -k\nabla T + P'J \quad (4)$$

where P' is the Peltier coefficient and J is the electric current flux.

$$P' = ST \quad (5)$$

$$J = -\sigma\nabla V - \sigma\alpha\nabla T \quad (6)$$

where σ is the electrical conductivity, k is thermal conductivity, V is electric scalar potential and α is the Seebeck coefficient.

Substituting Eq. (3) and Eq. (4) into Eq. (1) and Eq. (2);

$$\rho_d C_p \frac{\partial T}{\partial t} + \nabla \cdot (-k\nabla T + \alpha T(-\sigma\nabla V - \sigma\alpha\nabla T)) = (-\sigma\nabla V - \sigma\alpha\nabla T)(-\nabla V) \quad (7)$$

$$-\sigma(\nabla^2 V + \alpha\nabla^2 T) = \frac{\partial \rho_c}{\partial t} \quad (8)$$

The above equations can be used for both the steady state heating condition and the transient heating condition however, for the steady state heating condition,

$$\frac{\partial \rho_c}{\partial t} = 0 \quad (9)$$

3.1. Performance Equations

Considering the Seebeck effect, when a temperature difference is present, an open circuit voltage is generated which is given as [16]:

$$V_{oc} = \alpha\Delta T \quad (10)$$

where V_{oc} is the open circuit voltage, ΔT is the temperature difference across the TEG and α is the Seebeck coefficient.

When an external load resistor is connected to the TEG, the power output is expressed as

$$P_{out} = \left(\frac{\alpha\Delta T}{R_L + R_{in}} \right)^2 \times R_L \quad (11)$$

where R_L is the external load resistance and R_{in} is the TEG's internal resistance. Maximum power output can be obtained when $R_L = R_{in}$.

$$P_{out} = \frac{(\alpha\Delta T)^2}{4R_L} \quad (12)$$

Input power applied to the TEG hot side is given as

$$Q_{in} = q'' \times A \quad (13)$$

where q'' is the input heat flux and A is the TEG hot side surface area.

In this study, steady-state heating) and pulsed heating are applied to the TEG. Duty cycle and period time (τ) are used to characterize the pulsed heat flux. Duty cycle ($\frac{t^0}{\tau}$) is defined as the ratio of heating time (t^0) to period time. Throughout the simulations, the overall heat input in the pulsed heating case is equal to that of the steady state heating case. Rectangular and triangular functions are used to model the pulsed heat input flux the input heat flux for the rectangular function is given as [18]:

$$q'' = a + (b - a) \times \frac{t^0}{\tau} \quad (14)$$

For the triangular function, the input heat flux is given as [18]:

$$q'' = a + \frac{(b - a)}{2} \times \frac{t^0}{\tau} \quad (15)$$

where b/a is the ratio of maximum input heat flux to minimum input heat flux for a time period. Throughout this study, $b/a = 6$, $\frac{t^0}{\tau} = 0.1$, and $q'' = 20,000W \cdot m^{-2}$.

Considering six continuous time periods ($3\tau = 450s$), the transient heat input is given as

$$q'' = (b - a) \times f(t) + a \quad (16)$$

where $f(t)$ is the rectangular input function.

4. Results and Discussion

The results obtained from this study are shown in this section and discussed thereafter. Two pulsed heating functions are applied including rectangular and triangular pulsed heat. In addition, steady state heating is also analysed and compared to the transient pulsed heating. The numerical model used in this study has been verified by the authors in [3], [7] therefore, the results from this study can be trusted as accurate.

4.1. Influence of Transient and Steady State Heating

The influence of transient pulsed rectangular and triangular heating along with steady state heating on the performance of the TEG is shown in Fig. 2. As shown in Fig. 2, the rectangular pulsed heating provides the best performance for the TEG compared to triangular and steady state heating. Fig. 2a shows that the maximum hot side surface temperature of the TEG attains a value of 379.27K, 374.91K, 316.98K under rectangular, triangular and steady state heating respectively. This means that the temperature difference across the TEG under rectangular pulsed heating is maximum thus, its voltage and power output are the highest as shown in Fig. 2b and Fig. 2c respectively compared to the other heating conditions. Furthermore, it can be seen from Fig. 2 that both the rectangular and triangular pulsed heating enhanced the performance of the TEG significantly compared to the steady state heating. In fact, the maximum power output of the TEG under rectangular pulsed heating is the highest. The temperature and voltage distribution in the TEG are shown in Fig. 3. As expected, the highest temperature is achieved at the hot surface of the TEG where the heat flux is applied while the current flow from left to right in the TEG due to the ground position.

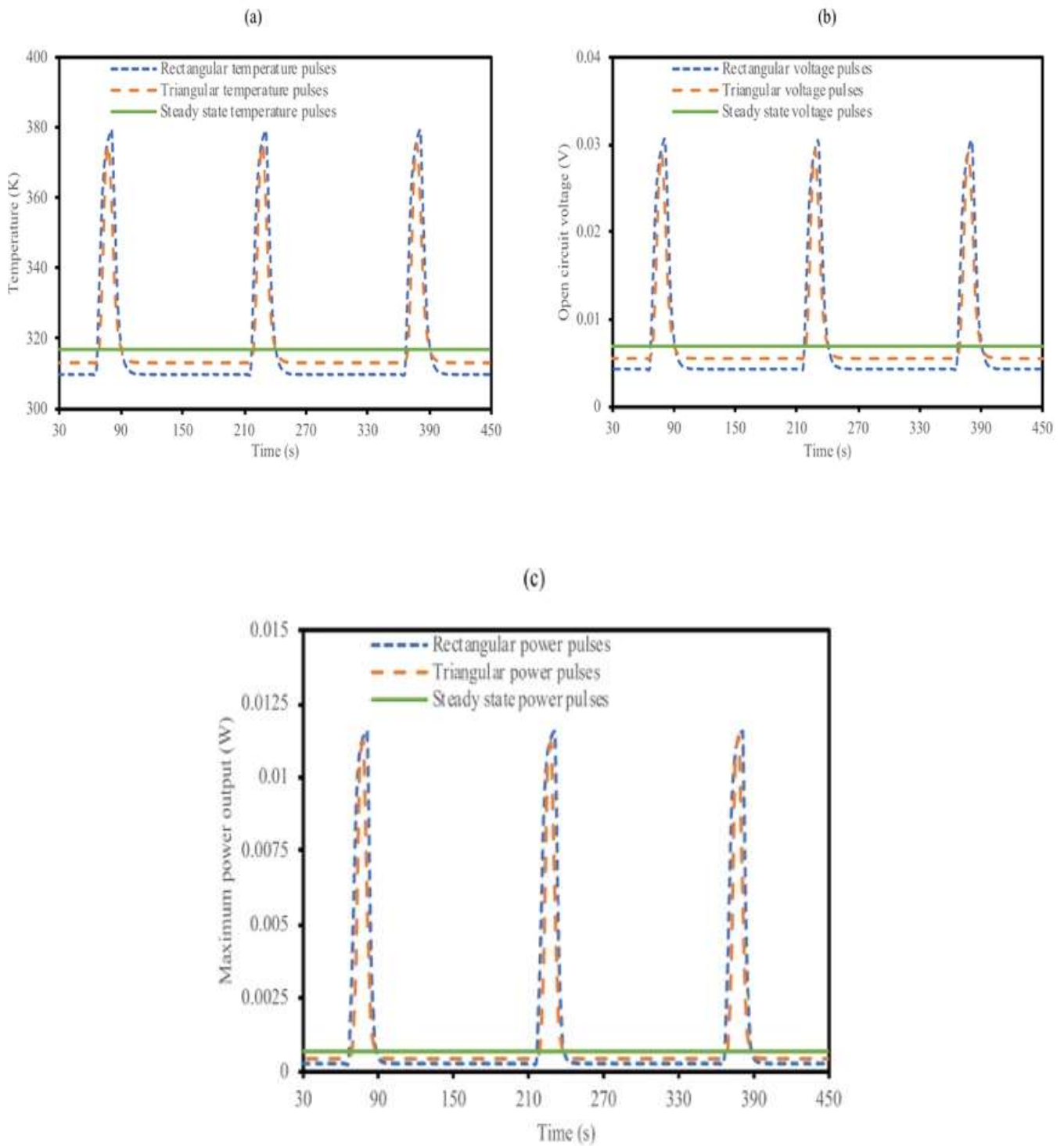


Fig. 2: Transient and steady state response of the TEG (a) temperature (b) open circuit voltage and (c) maximum power output.

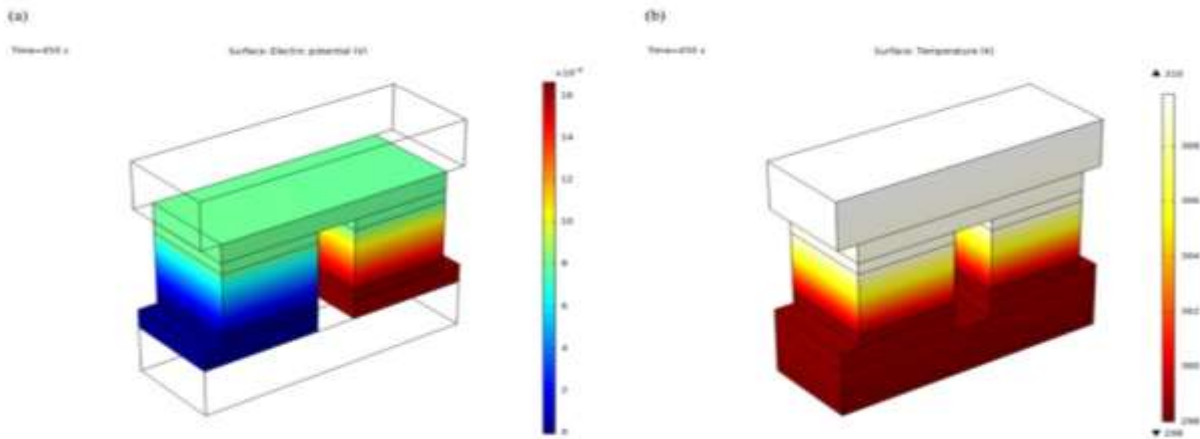


Fig. 3: Distribution of (a) voltage and (b) temperature in the TEG.

4.2. Influence of Thermoelectric Leg Length and Area

Since Fig. 2 already showed that the rectangular pulsed heating provides the best performance, it is used to study the influence of thermoelectric leg height and area on the performance of the TEG. Therefore, Fig. 3 shows the variation of leg length and area with the maximum power output of the TEG. It can be clearly seen that the power output of the TEG decreases as the leg height increased thus, this resonates the argument that shorter thermoelectric leg length provides enhanced power output. In addition, it can be seen that the power output of the TEG increases as the cross-sectional area of the leg increases. Again, this is an expected and normal phenomenon. This results therefore show the vital importance of optimizing the geometry of thermoelectric generators as it greatly influences its performance.

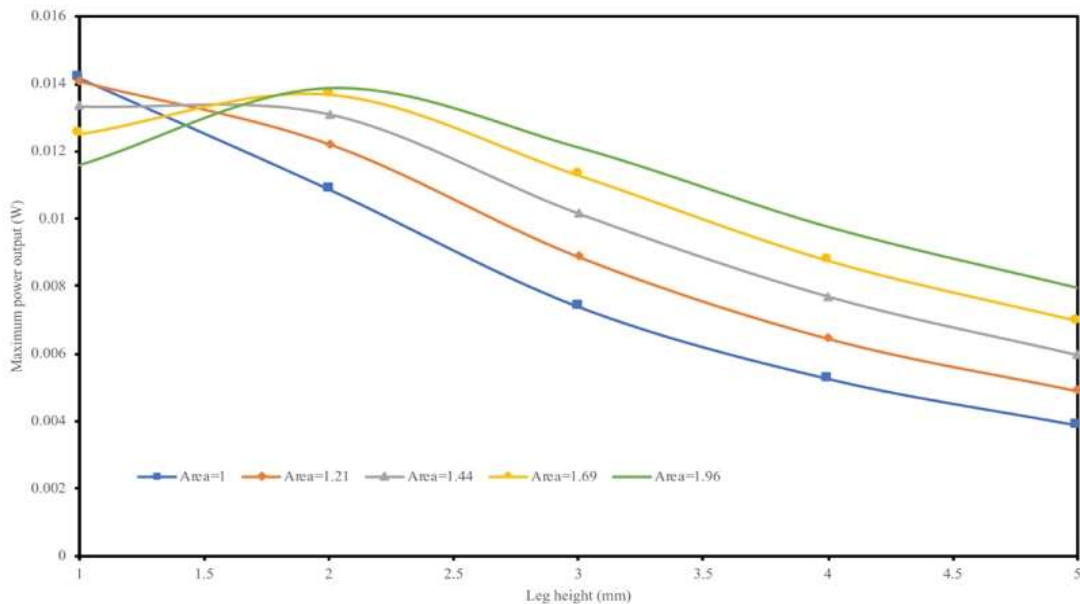


Fig. 4: Maximum power output variation with leg height and area under rectangular pulse at 81s.

5. Conclusion

This study presented a detailed numerical investigation on the thermal and electrical performance of a thermoelectric generator under transient pulsed and steady state heating conditions. Rectangular and triangular pulsed heating functions were applied alongside steady state heating and the results obtained from the different heating conditions were compared. A three-dimensional numerical model was utilized in this study and COMSOL 5.4 Multiphysics software was the chosen software. In addition, finite element method was utilized to solve the heat transfer equations and temperature dependent thermoelectric material properties were considered. The influence of transient and steady state heating on the performance of the TEG was studied and geometry optimization study was performed. Results showed that rectangular pulsed heating significantly enhanced the performance of the TEG compared to triangular and steady state heating. In fact, both transient pulsed heating greatly increased the power output of the TEG compared to the steady state heating. Also, the power output of the TEG decreased as the leg height increased however, it increased as the leg area increased. Therefore, shorter thermoelectric legs with wider cross-sectional area are suggested to enhance the performance of the TEG.

Acknowledgements

The first author would like to acknowledge the PhD studentship received from the University of Hull and the financial support received from Energy Technologies Research Group at the University of Hull.

References

- [1] T. M. O. Diallo, M. Yu, J. Zhou, X. Zhao, S. Shittu, G. Li, J. Ji, D. Hardy, "Energy performance analysis of a novel solar PVT loop heat pipe employing a microchannel heat pipe evaporator and a PCM triple heat exchanger," *Energy*, vol. 167, pp. 866–888, 2019.
- [2] G. Li, S. Shittu, T. M. O. Diallo, M. Yu, X. Zhao, and J. Ji, "A review of solar photovoltaic-thermoelectric hybrid system for electricity generation," *Energy*, vol. 158, pp. 41–58, Sep. 2018.
- [3] S. Shittu, G. Li, X. Zhao, X. Ma, Y. G. Akhlaghi, and E. Ayodele, "High performance and thermal stress analysis of a segmented annular thermoelectric generator," *Energy Convers. Manag.*, vol. 184, pp. 180–193, 2019.
- [4] S. B. Riffat and X. Ma, "Thermoelectrics: A review of present and potential applications," *Appl. Therm. Eng.*, vol. 23, no. 8, pp. 913–935, 2003.
- [5] D. Champier, "Thermoelectric generators: A review of applications," *Energy Convers. Manag.*, vol. 140, pp. 167–181, 2017.
- [6] J. Xiao, T. Yang, P. Li, P. Zhai, and Q. Zhang, "Thermal design and management for performance optimization of solar thermoelectric generator," *Appl. Energy*, vol. 93, pp. 33–38, 2012.
- [7] S. Shittu, G. Li, X. Zhao, and X. Ma, "Series of detail comparison and optimization of thermoelectric element geometry considering the PV effect," *Renew. Energy*, vol. 130, pp. 930–942, 2019.
- [8] G. Li, S. Shittu, X. Ma, and X. Zhao, "Comparative analysis of thermoelectric elements optimum geometry between Photovoltaic-thermoelectric and solar thermoelectric," *Energy*, vol. 171, pp. 599–610, 2019.
- [9] G. Li, X. Zhao, Y. Jin, X. Chen, J. Ji, and S. Shittu, "Performance Analysis and Discussion on the Thermoelectric Element Footprint for PV–TE Maximum Power Generation," *J. Electron. Mater.*, vol. 47, no. 9, pp. 5344–5351, 2018.
- [10] G. J. Snyder, "Application of the compatibility factor to the design of segmented and cascaded thermoelectric generators," *Appl. Phys. Lett.*, vol. 84, no. 13, pp. 2436–2438, 2004.
- [11] M. H. Elsheikh, D. A. Shnawah, M. F. M. Sabri, S. B. M. Said, M. H. Hassan, M. B. A. Bashir, M. Mohamad "A review on thermoelectric renewable energy: Principle parameters that affect their performance," *Renew. Sustain. Energy Rev.*, vol. 30, pp. 337–355, 2014.
- [12] S. Omer and D. Infield, "Design optimization of thermoelectric devices for solar power generation," *Sol. Energy Mater. Sol. Cells*, vol. 53, pp. 67–82, 1998.
- [13] C. Hadjistassou, E. Kyriakides, and J. Georgiou, "Designing high efficiency segmented thermoelectric generators," *Energy Convers. Manag.*, vol. 66, pp. 165–172, 2013.

- [14] A. B. Zhang, B. L. Wang, D. D. Pang, J. B. Chen, J. Wang, and J. K. Du, "Influence of leg geometry configuration and contact resistance on the performance of annular thermoelectric generators," *Energy Convers. Manag.*, vol. 166, no. March, pp. 337–342, 2018.
- [15] D. N. Kossyvakis, G. D. Voutsinas, and E. V. Hristoforou, "Experimental analysis and performance evaluation of a tandem photovoltaic-thermoelectric hybrid system," *Energy Convers. Manag.*, vol. 117, pp. 490–500, 2016.
- [16] L. Chen and J. Lee, "Effect of pulsed heat power on the thermal and electrical performances of a thermoelectric generator," *Appl. Energy*, vol. 150, pp. 138–149, 2015.
- [17] F. Meng, L. Chen, and F. Sun, "Effects of temperature dependence of thermoelectric properties on the power and efficiency of a multielement thermoelectric generator," *Int. J. Energy Environ.*, vol. 3, no. 1, pp. 137–150, 2012.
- [18] S. Asaadi, S. Khalilarya, and S. Jafarmadar, "Numerical study on the thermal and electrical performance of an annular thermoelectric generator under pulsed heat power with different types of input functions," *Energy Convers. Manag.*, vol. 167, no. January, pp. 102–112, 2018.